Silver Coated Microstrip Antenna Array

K. Prahlada Rao[1], Vani R. M.[2], and P. V. Hunagund[1]
[1] Dept. of PG Studies and Research in Applied Electronics, Gulbarga University, Gulbarga, India
[2] University Science Instrumentation Center, Gulbarga University, Gulbarga, India
Email: pra_kaluri@rediffmail.com

***Abstract*—The paper provides insight into the effect of electromagnetic band gap structures, defective ground structures and nano film deposition on microstrip antenna array. The modified microstrip antenna array provides overall bandwidth and reduced mutual coupling of 254.7 %, –31.29, –30.78 and –33.20 dB respectively. In addition a high gain of 15.03 dB is also obtained. The modified microstrip antenna array is also producing good radiation characteristics in the form of reduced back lobe radiation. On the other hand the conventional microstrip antenna array produces bandwidth, gain and mutual coupling of 4.89 %, 6.81, –16.95, –14.22 and –17.30 dB respectively. The fundamental resonant frequency of conventional microstrip antenna array is 5.53 GHz. FR-4 glass epoxy is employed as the dielectric substrate. The microstrip antenna arrays are designed using Mentor Graphics IE3D software.**

***Index Terms*—corporate feeding technique, gain, microstrip antenna array, mutual coupling, radiation pattern, return loss.**

I. Introduction

More data transfer, better size reduction and selection of the appropriate substrate are the key aspects of antenna designers. Microstrip antennas have a radiating patch which is placed on top of dielectric substrate and a ground plane below the dielectric substrate. In the past few years Electromagnetic Band Gap (EBG) structures and Defective Ground Structures (DGS) have been proved to be the best champions of microstrip antennas in improving the performance of these antennas. EBG structures have uniformly arranged unit cells which are capable of reducing the impact of surface waves which are produced in the substrate layer. DGS are defects where part of the copper is removed from the finite ground plane. [1]-[5].

In [6] authors have presented microstrip antenna arrays with novel EBG structures integrated in the ground plane. It has been demonstrated that the performance of microstrip antenna arrays has been enhanced to a certain extent. In [7] T shaped DGS was implemented to reduce the side lobe level and mutual coupling. The mutual coupling is reduced by 8 dB in the E plane and by 9 dB in the H plane between the two adjacent patches when compared in the absence of DGS. In [8] authors have used inter digital resonator to reduce the mutual coupling between the elements of antenna array designed at 2.4 GHz. The feeding network is in the form of CRLH-TL based phase shifter and T junction based power divider. An impedance bandwidth of 8.34 % is obtained. In [9] authors have employed dumbbell shape DGS structure to reduce the mutual coupling from −32.91 to −39.88 dB respectively. In [10] the use of dumbbell shape DGS has produced a peak gain of 6.54 dB with good return losses at the three resonant frequencies −3.72, 4.76 and 7.63 GHz respectively. The spacing between the two antenna elements is 80 mm. The directivity and antenna efficiency are also improved. In [11] authors have designed miniaturized antenna array using DGS structure. A virtual size reduction of 43.75 % is achieved. However, there is a decrease in gain value after the introduction of DGS. In [12] authors have achieved higher gain and bandwidth of 8.96 dB and 1.652 GHz after the introduction of DGS. In the absence of DGS, the gain and bandwidth are equal to 4.38 and 675 MHz respectively. A miniaturization of 78.97 % is also achieved. In [13] authors have achieved a gain of 11.76 dB in the presence of L shaped slot loading T shaped slot EBG structure in between the elements of the microstrip antenna array. Sound reduction in mutual coupling and increase in bandwidth contribute to the enhanced performance of 2×2 microstrip antenna array. The antenna elements are fed by probe feed technique. In [14] the presence of EBG structure has increased the bandwidth from 170 to 190 MHz. The modified antenna array is applicable for WLAN frequency band. Higher values of gain and directivity with reduction in mutual coupling confirm the capability of EBG structures. In [15] authors have designed microstrip antenna array with Sierpenski radiating patches. With Sierpenski fractal radiating patch, good improvement in gain and bandwidth are obtained. In [16] author has discussed the application of EBG structures as band pass filters for ultra wide band. In [17] authors have designed uniplanar EBG structure to enhance the performance of microstrip antenna array. With the increase in gap width between the EBG unit cells from 1 to 2 mm, there is considerable increase in bandwidth and gain. Antenna gain for 1 and 2 mm gap width are 4.75 and 5.29 dB respectively. In [18] authors have experimented by depositing iron nano particles on top of radiating patch of microstrip antenna. An enhanced bandwidth of 26.02 % has been obtained. In [19] microstrip antenna with equally spaced nano dots deposited on the epoxy resin is designed to produce multi bands frequencies. An impedance bandwidth of 2-3 GHz has been obtained at the resonant frequency. In [20] authors have designed microstrip antenna with zinc nano

Manuscript received January 20, 2019; revised April 8, 2019; accepted April 8, 2019.
Corresponding author: K. Prahlada Rao (email: pra_kaluri@rediffmail.com).

©2019 Int. J. Elec. & Elecn. Eng. & Telcomm.

doi: 10.18178/ijeetc.8.5.281-286

particles loaded on the radiating patch. A healthy bandwidth and gain have been obtained.

The newness in this paper is the usage of EBG structures both in the ground plane and on the surface of microstrip antenna arrays. Additionally, silver material of nano thickness is deposited on top of entire copper area.

II. Conventional Microstrip Antenna Array

The design process of microstrip antenna arrays starts with the design of Conventional Microstrip Antenna Array (CMAA). CMAA is designed at 6 GHz. CMAA consists of four identical radiating patches which are rectangular in shape. The dimensions of each of the radiating patches of CMAA are 15.73 mm × 11.76 mm. The dimensions of all the parts of CMAA are calculated as per the formulae available in the literature review. The distance between the four adjacent radiating patches is equal to $\lambda/4$. λ is the wavelength calculated as the design frequency of 6 GHz. The height of the substrate used is 1.6 mm. The dielectric constant and loss tangent of FR-4 glass epoxy substrate are 4.2 and 0.0245 respectively. The schematic of CMAA is depicted in Fig. 1. All the dimensions of CMAA are tabulated in Table I.

The schematic shown in Fig. 1 is employed to determine return loss, resonant frequency and bandwidth. However to measure the parameter mutual coupling between the radiating elements, the four radiating elements of CMAA are excited individually as shown in Fig. 2. The separation between the adjacent antenna elements of setup of CMAA depicted in Fig. 2 is same as that in Fig. 1.

Table I. Parameter Values of CMAA

Parameter	Value (mm)
Length of the patch (L_p)	15.73
Width of the patch (W_p)	11.76
Length of the quarter wave transformer (L_t)	6.47
Width of the quarter wave transformer (W_t)	0.47
Length of the 50Ω line (L_1)	6.52
Width of the 50Ω line (W_1)	3.05
Length of the coupler (L_c)	3.05
Width of the coupler (W_c)	3.05
Length of the 70Ω line (L_2)	6.54
Width of the 70Ω line (W_2)	1.62
Length of the 100Ω line (L_3)	6.56
Width of the 100Ω line (W_3)	0.70
Length of the feed line (L_f)	6.52
Width of the feed line (W_f)	3.05

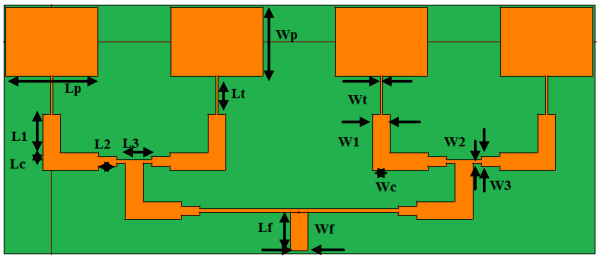

Fig. 1. Schematic of CMAA.

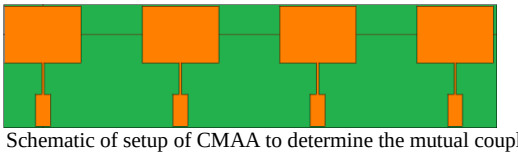

Fig. 2. Schematic of setup of CMAA to determine the mutual coupling.

III. Modified Microstrip Antenna Array

The ground plane and surface of CMAA are changed to design the Modified Microstrip Antenna Array (MMAA). The ground plane and surface of MMAA consists of DGS and EBG structures. The schematic of unit cell of EBG structure of MMAA is shown in Fig. 3.

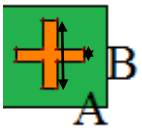

Fig. 3. Schematic of unit cell of EBG structure of MMAA.

The unit cell of EBG structure of MMAA is plus shape patch type. It has dimensions of A and B where A = 5 mm and B=0.5 mm respectively. The EBG structure employed to design MMAA is shown in Fig. 4.

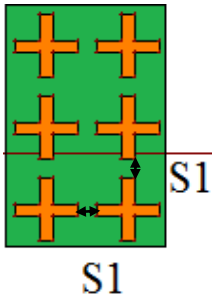

Fig. 4. Schematic of EBG structure of MMAA.

The EBG structure depicted in Fig. 4 is an array of plus shape patch type unit cells. The two dimensional structure consists of 2 columns and 3 rows of plus shape patch type unit cells. The unit cells of the EBG structure of MMAA are separated by distance of 1.5 mm. In Fig. 4 the periodicity is represented by S_1.

The DGS structure etched in the ground plane of MMAA is shown in Fig. 5. In Fig. 5 P =4 mm, Q = 1.1 mm, R = 4 mm and S = 1.9 mm respectively.

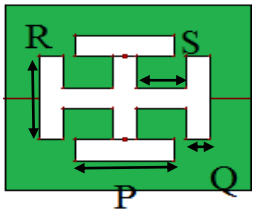

Fig. 5. Schematic of DGS of MMAA.

In addition a thin layer of silver is placed on top of copper layer. The thickness of silver coating is equal to 30 nm. The schematic of MMAA is depicted in Fig. 6. The portion of schematic represented in grey color indicates the silver coating on top of copper metal.

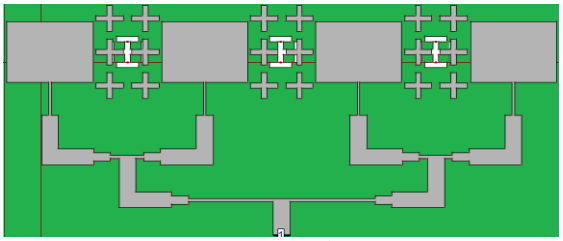

Fig. 6. Schematic of PMAA.

The schematic of setup of radiating elements of MMAA used to estimate the mutual coupling between the antenna elements is depicted in Fig. 7. The grey portion of the schematic represents the silver deposition on top of copper metal.

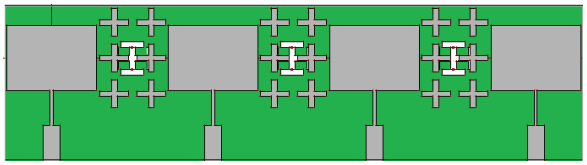

Fig. 7. Schematic of setup of PMAA to determine the mutual coupling.

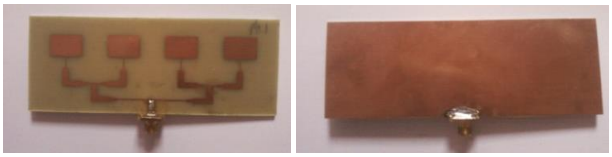

(a) Front view (b) Rear view

Fig. 8. Photograph of CMAA.

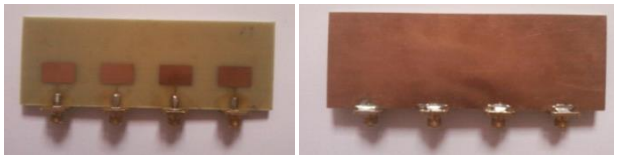

(a) Front view (b) Rear view

Fig. 9. Photograph of setup of CMAA for mutual coupling measurement.

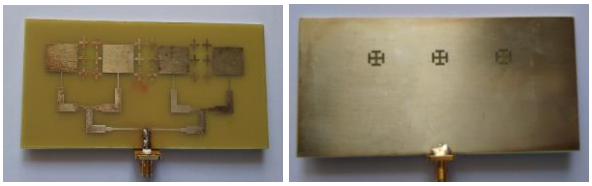

(a) Front view (b) Rear view

Fig. 10. Photograph of MMAA.

(a) Front view (b) Rear view

Fig. 11. Photograph of setup of MMAA for mutual coupling measurement.

IV. Fabrication of Antenna Arrays

The next step after designing the antenna arrays is fabrication. The artwork of the antenna array designs is obtained using AUTOCAD – 2004. A laser print out of the artwork is then taken. The dimensions are achieved on one side of the printed circuit board using photolithographic process. An enlarged artwork is prepared on Stabiline or Rubylith film. Using the precision cutting blade the opaque layer of the Stabiline or Rubylith film is cut as per the geometrical dimensions and can be removed to produce a positive or negative representation of the schematic.

The laminate is cleared using the recommended substrate to confirm proper adhesion of the photo resist. Later the photo resist is applied to both sides of the laminate using laminator. The photographic negative is linked in very close contact with the polyethylene cover sheet of the photo resist. Further with the exposure to proper wavelength of light, polymerization of the exposed photo resist occurs. The both sides of photo resist are exposed completely without a mask as the copper is retained to act as a ground plane. The photo resist is removed from the polyethylene cover sheet and the antenna is developed in a developer.

Visual and optical inspection is performed to ensure a good product. The edges of the product are smoothened and the product (antenna) is reinserted in water and dried. Dowel pins are employed for alignment and the assembly is heated under pressure. The assembly is allowed to cool down under pressure and the laminate is removed for inspection.

Finally a coating of silver is deposited on top of entire copper area by dipping the product (antenna) in a tank of silver solution. The entire assembly is allowed to cool to ensure silver is deposited properly.

Fig. 8, Fig. 9, Fig. 10, and Fig. 11 depict the photographs of the fabricated antenna arrays.

V. Measured Results and Discussion

The antenna arrays CMAA and MMAA are compared in terms of various parameters. The measured results are obtained using vector network analyzer. The graphs of return loss and mutual coupling versus frequency of CMAA are depicted in Fig. 12, Fig. 13, and Fig. 14, respectively.

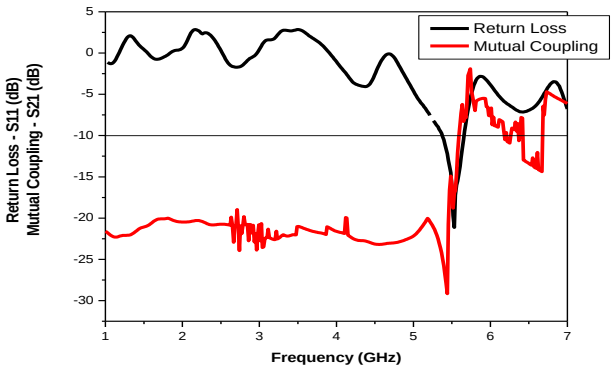

Fig. 12. Graph of return loss and mutual coupling: S_{21} vs frequency of CMAA.

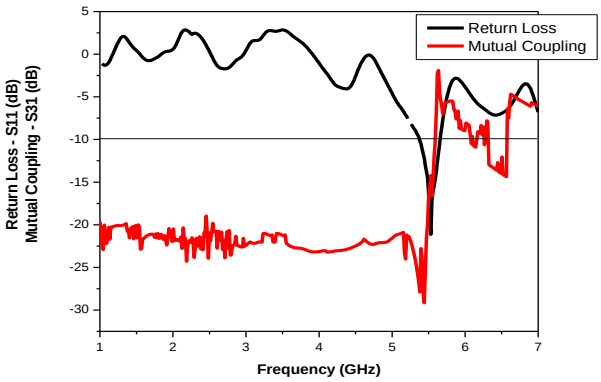

Fig. 13. Graph of return loss and mutual coupling: S_{31} vs frequency of CMAA.

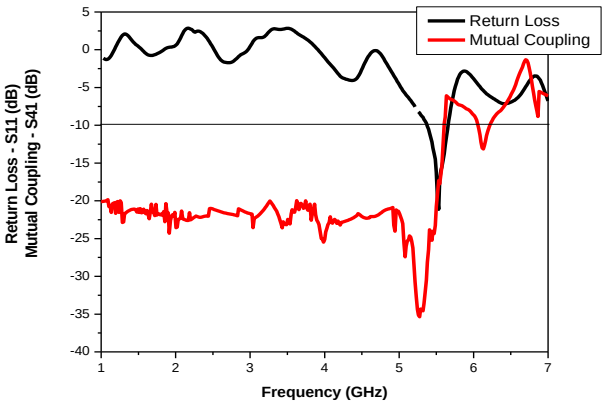

Fig. 14. Graph of return loss and mutual coupling: S_{41} vs frequency of CMAA.

The graphs in Fig. 12, Fig. 13, and Fig. 14 show that CMAA is resonating at the fundamental frequency of 5.53 GHz. The return loss produced at the resonant frequency of 5.53 GHz is equal to −21.06 dB. From the return loss graph the parameter bandwidth is calculated. The lower frequency is subtracted from upper frequency where the return loss is equal to – 10 dB. The lower and upper frequencies are located on either side of the resonant frequency. Therefore the bandwidth of CMAA is equal to 273 MHz. The bandwidth (%) is determined by using (1)

$$\frac{\text{Bandwidth}}{\text{Resonant frequency}} \times 100\% \quad (1)$$

Hence CMAA is producing bandwidth of 4.89 %. As the bandwidth of CMAA is very narrow it is very much required to enhance it.

From Fig. 12, Fig. 13, and Fig. 14 we see that the measured values of mutual coupling (S_{21}, S_{31} and S_{41}) are −16.95, −14.22 and −17.30 dB respectively. The values of mutual coupling are very high and need to be decreased. Additionally we can see that the graphs of return loss and mutual coupling versus frequency are crossing each other at the resonant frequency of 5.53 GHz. This means that there is interference between the transmitting element 1 and the receiving elements 2, 3 and 4 respectively. Hence there is no proper transmission and reception of information between the transmitting element 1 and the receiving elements 2, 3 and 4.

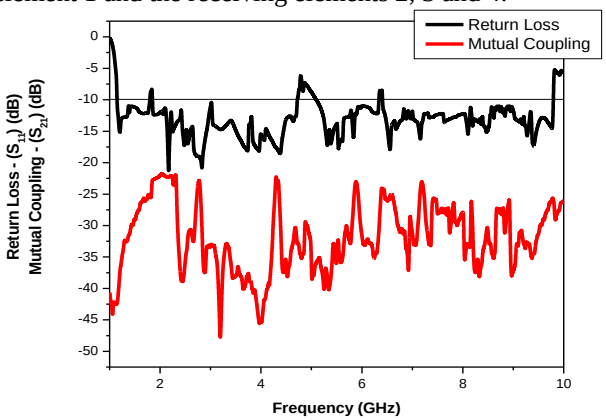

Fig. 15. Graph of return loss and mutual coupling: S_{21} vs frequency of MMAA.

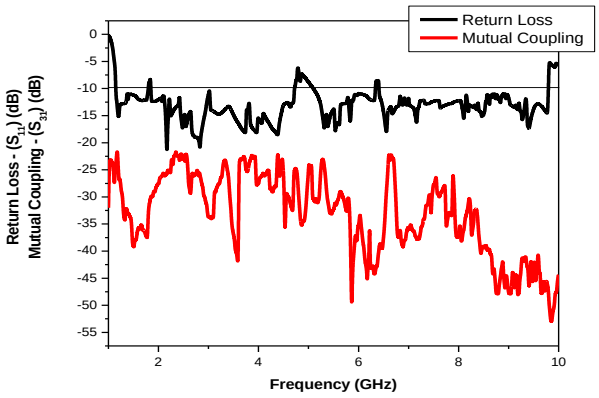

Fig. 16. Graph of return loss and mutual coupling: S_{31} vs frequency of MMAA.

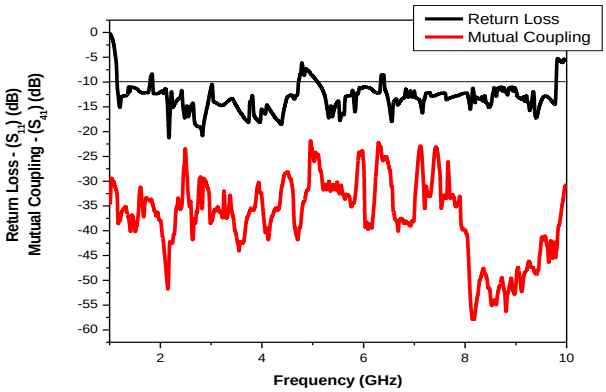

Fig. 17. Graph of return loss and mutual coupling: S_{41} vs frequency of MMAA.

The graphs of return loss and mutual coupling versus frequency of MMAA are shown in Fig. 15, Fig. 16 and Fig. 17, respectively.

Fig. 15, Fig. 16, and Fig. 17 depict that MMAA is resonating at 1.19, 2.11, 5.53 and 6.35 GHz respectively. The return losses produced at these resonant frequencies are −15.14, −21.27, −17.82 and −17.88 dB respectively. The individual bandwidths measured at these resonant frequencies are 640, 2870, 1220 and 3360 MHz respectively. Thus the overall bandwidth of MMAA is equal to 254.7 %. Hence MMAA is a better antenna than CMAA in terms of overall bandwidth (%) as the bandwidth is enhanced from a mere 4.89 to 254.7 %. In addition the values of mutual coupling are reduced to -31.29, −30.78 and −33.20 dB respectively. Moreover, Figs. 15, 16 and 17 also depict that the graphs of return loss and mutual coupling are no more overlapping at the resonant frequency of 5.53 GHz. This implies that interference is decreased between the transmitting element 1 and the receiving elements 2, 3 and 4 respectively. Therefore there is improved transfer of electromagnetic waves between the transmitting element 1 and the receiving elements 2, 3 and 4 respectively. Hence MMAA is a better candidate than CMAA in terms of mutual coupling.

Gain is another important parameter employed to evaluate the performance of microstrip antenna arrays. The gain of a microstrip antenna array is calculated by using the equation (2)

$$G = 20\log_{10}\left(\frac{4\pi R}{\lambda}\right) + 10\log_{10}\frac{P_r}{P_t} - G_t \quad (2)$$

In (2) R is the distance between the transmitting antenna and the antenna under test. The transmitting antenna employed is the standard pyramidal horn antenna. λ is the wavelength calculated at the resonant frequency of 5.53 GHz. P_r and P_t are the received and transmitted powers. And G_t is the gain of transmitting antenna.

The parameter R is calculated by using (3)

$$R \geq \frac{2D^2}{\lambda} \quad (3)$$

In (3) D is the largest dimension of the standard pyramidal horn antenna. The length and breadth of the standard pyramidal horn antenna are equal to 24 and 14 cm respectively. Hence the value of D is equal to 24 cm. Substituting the values of relevant parameters in (3), the value of R is equal to 71.86 m.

The parameter gain of the transmitting antenna is calculated by using (4)

$$G_t = 10\log_{10} G_s \quad (4)$$

where

$$G_s = \frac{2\pi ab}{\lambda^2} \quad (5)$$

In (5) a and b are the length and breadth of standard pyramidal horn antenna.

Initially considering CMAA as receiving antenna, the transmitted and received powers are equal to 8.7 µW and 12.414 nW respectively. Using (2) the gain of CMAA is calculated as equal to 6.81 dB. Next considering MMAA as the receiving antenna, the corresponding transmitted and received powers are equal to 8.7 µW and 81.46 nW. Hence the calculated gain of MMAA is equal to 15.03 dB. Hence with the introduction of plus shape patch type EBG structure, DGS structure and silver film of 30 nm thickness, the gain of CMAA is increased from 6.81 to 14.98 dB. Hence MMAA is a better performer than CMAA in terms of gain parameter.

Fig. 18 depicts the radiation patterns of CMAA and MMAA. From Fig.18 we see that at the angle of 90^0 forward power is measured and at the angle of 270^0 backward power is measured. The measured values of forward and backward powers of CMAA are equal to -2 and -4.5 dB respectively. MMAA is producing the forward and backward powers equal to -0.5 and -5 dB respectively. Comparing the forward powers of CMAA and MMAA, MMAA is radiating excess power of 1.5 dB than its counterpart i.e. CMAA. As far as the undesired power is concerned, the back lobe radiation is decreased by 0.5 dB in the case of MMAA. Hence MMAA is a performing superiorly than CMAA in terms of forward and backward powers.

The parameter Front to back ratio (FBR) is evaluated by deducting the backward power from the forward power. Therefore the calculated values of FBR of CMAA and MMAA are equal to 2.5 and 4.5 dB respectively. The higher value of FBR of MMAA than CMAA means that MMAA is radiating more effectively in the wanted and unwanted directions. Hence MMAA is a better antenna than CMAA in terms of CMAA.

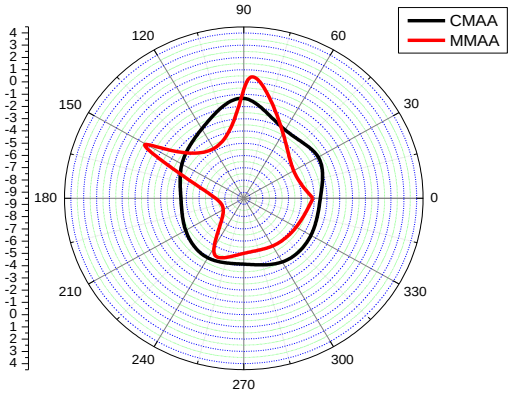

Fig. 18. Radiation plots of CMAA and MMAA.

From Fig. 12, Fig. 13, and Fig. 14 we see that CMAA is resonating at the fundamental frequency of 5.53 GHz. From Fig. 15, Fig. 16, and Fig. 17 we see that MMAA is resonating at the fundamental frequency of 1.19 GHz. This implies that MMAA is resonating at a fundamental resonant frequency which is lesser than that of CMAA. This corresponds to virtual size reduction. The parameter virtual size reduction (%) is calculated by using the (6)

$$\left(\frac{f_a - f_b}{f_a}\right) \times 100 \quad (6)$$

where f_a and f_b are the fundamental resonant frequencies of CMAA and MMAA. Hence the virtual size reduction obtained with the help of MMAA is 78.48 %.

VI. Summary of Measured Results

Table II depicts the summarized measured results.

TABLE II. SUMMARIZED MEASURED RESULTS

Type of antenna/parameter	CMAA	MMAA
Resonant frequency (GHz)	5.53	1.19 2.11 5.53 6.35
Return loss (dB)	-21.06	-15.14 -21.27 -17.82 -17.88
Bandwidth (MHz)	273	640 2870 1220 3360
Bandwidth (%)	4.89	254.7
Gain (dB)	6.81	15.03
Mutual coupling – S_{21}, S_{31}, S_{41} (dB)	-16.95 -14.22 -17.30	-31.44 -36.41 -31.62
FBR (dB)	2.5	4.5

VII. Conclusion

An attempt to design and fabricate the four element microstrip antenna array in the presence of EBG, DGS and silver metal deposition is successfully executed. Both

the conventional and modified microstrip antenna arrays are experimentally tested and measured results confirm the better performance of modified microstrip antenna array over its counterpart. An overall bandwidth of 254.7 %, enhanced gain of 15.03 dB coupled with good reduction in mutual coupling are obtained.

REFERENCES

[1] R. Ludwig and P. Bretchko, *RF Circuit Design: Theory and Applications*, 2nd ed., 2009.

[2] C. A. Balanis, *Antenna Theory, Analysis and Design*, 2nd ed. John Wiley & Son, Inc., 1997.

[3] I. J. Bahl and P. Bhartia, *Microstrip Antennas*, Artech House, 1980.

[4] F. Yang and Y. Rahmat-Samii, *Electromagnetic Band Gap Structures in Antenna Engineering*, Cambridge University Press, 2009.

[5] C. G. Christodoulou and P. F. Wahid, *Fundamentals of Antennas: Concepts and Applications*, Prentice Hall of India, 2004.

[6] D. N. Elsheakh, E. A. Abdallah, M. F. Iskander, and H. A. Elsadek, "Microstrip antenna array with new 2D-electromagnetic band gap structure shapes to reduce harmonics and mutual coupling," *Progress in Electromagnetic Research*, vol. 12, pp. 203-213, Jan. 2010.

[7] S. Viesse, S. Asadi, and M. K. Hedayati, "A novel compact defected ground structure and its application in mutual coupling reduction of a microstrip antenna," *Turkish Journal of Electrical Engineering and Computer Science*, vol. 24, pp. 3664-3670, 2016.

[8] W. Qiao, X. Gao, X. Y. Yu, S. M. Li, Y. N. Jiang, and H. F. Ma, "Ultra-compact microstrip antenna array and miniaturized feeding network," *Progress in Electromagnetic Research C*, vol. 71, pp. 111-122, 2017.

[9] S. Gharat and P. P. Narwade, "Defected ground structure – based microstrip antenna arrays with reduced mutual coupling," *Int. Research Journal of Engineering and Technology*, vol. 3, no. 5, pp. 2710-2715, May 2016.

[10] Roopali, P. Mishra, and Shalini, "Calculation of performance parameters of DGS structured micro-strip antenna array," *Int. Journal of Electronics, Electrical and Computational System*, vol. 4, no. 8, pp. 14-21, Aug. 2015.

[11] O. Oulhaj, N. A. Touhami, M. Aghoutane, and A. Tazon, "A miniature microstrip patch antenna array with defected ground structure," *Int. Journal of Microwave and Optical Technology*, vol. 11, no. 1, pp. 32-39, Jan. 2016.

[12] M. Kumar and V. Nath, "Analysis of low mutual coupling compact multi-band microstrip patch antenna and its array using defected ground structure," *Engineering Science and Technology*, vol. 19, pp. 866-874, 2016.

[13] H. S. Gally, Z. A. Ahmed, and A. H. Abood, "Surface wave minimizing in 2×2 microstrip antenna array," *Journal of Natural Sciences Research*, vol. 8, no. 10, pp. 67-73, 2018.

[14] C. K. Ghosh, B. Rana, and S. K. Parui, "Performance enhancement of microstrip patch antenna array with EBG structure," *Int. Journal of Electronics and Communication Technology*, vol. 2, no. 4, pp. 280-283, Dec. 2011.

[15] M. Gupta and V. Mathur, "Sierpinski array with swastika electromagnetic band gap for Ku – band applications," *Indian Journal of Science and Technology*, vol. 9, no. 32, pp. 1-7, Aug. 2016.

[16] D. S. Raja, "Periodic EBG structure based UWB band pass filter," *Int. Journal of Advanced Research in Electrical, Electronics and Instrumentation Engineering*, vol. 2, no. 5, pp. 1682-1686, May 2013.

[17] S. Bhavsar and B. Singh, "Microwave patch arrays with EBG effect of changing gap," *Int. Journal of Advanced Research in Electrical, Electronics and Instrumentation Engineering*, vol. 2, no. 8, pp. 3734-3737, Aug. 2016.

[18] C. P. Mahesh, P. Mali, M. Sharon, and M. Sharon, "Enhancement of bandwidth of equilateral triangular microstrip antenna using nanoparticles," *Int. Journal for Research in Applied Science & Engineering Technology*, vol. 6, no. 5, pp. 257-3737, 2018.

[19] J. V. Chauhan, A. Kandwal, and S. K. Khah, "High frequency multilayer equally spaced nano dot antenna array," *Int. Journal of Emerging Technology and Advanced Engineering*, vol. 4, pp. 336-338, 2014.

[20] C. P. Mahesh, P. Mali, M. Sharon, and M. Sharon, "Design and fabrication of rectangular using Zinc nanoparticles for wireless applications and enhancement of bandwidth," *Int. Journal for Research in Applied Science & Engineering Technology*, vol. 6, no. 5, pp. 249-252, 2018.

K. Prahlada Rao is currently pursuing Ph.D. on full time basis in Dept. of Applied Electronics, Gulbarga University, Gulbarga, India. Prahlada's areas of research interests include microstrip antennas and arrays, electromagnetic band gap structures, defective ground structures, nano films.

He has published many papers in various national and international conferences and journals like Springer, Elsevier, IEEE, Scopus, Web of Science etc. He is a life member of Indian Society for Technical Education.

Vani R. M received B.E. in Electrical and Electronics from B.I.E.T, Davangere and M. Tech in Industrial Electronics from S.J.C.E. Mysore, Karnataka. She has received Ph.D. in Applied Electronics from Gulbarga University, Gulbarga, India, in the year 2005. She is working as Professor and Head, University Science Instrumentation Centre, Gulbarga University, Gulbarga, India.

She has more than 100 research publications in national and international reputed journals/Conference proceedings. She has presented many research papers in National/ International conferences in India and abroad. She has guided many Ph.D. and M.Phil. students. She has conducted several courses, workshops and symposiums for the benefit of university faculty and PG students. Her areas of interest are microwave antennas, compact and broadband antennas, embedded controllers and Wireless communication. She has completed one UGC major research project.

P. V. Hunagund, received M. Sc and Ph.D. from the Dept. of Applied Electronics, Gulbarga University, Gulbarga, in the year 1982 and 1992 respectively. Hunagund is working as professor in Dept. of Applied Electronics, Gulbarga University, Gulbarga, India.

He has more than 125 research publications in national and international reputed journals, more than 100 research publications in national and international symposium/Conferences. He has presented many research papers in National/International conferences in India and abroad. He has guided many Ph.D. and M. Phil. students. He has completed three major research projects funded by AICTE, DST and UGC New Delhi.